

High Structural Complexity of Potassium Uranyl Borates Derived from High-Temperature/High-Pressure Reactions

Shijun Wu,^{†,‡,§} Shuao Wang,^{†,||,¶} Matthew Polinski,[⊥] Oliver Beermann,[‡] Philip Kegler,[‡] Thomas Malcherek,[▽] Astrid Holzheid,[‡] Wulf Depmeier,[‡] Dirk Bosbach,[§] Thomas E. Albrecht-Schmitt,^{*,⊥,#} and Evgeny V. Alekseev^{*,§,§}

[†]Guangzhou Institute of Geochemistry, Chinese Academy of Sciences, 511 Kehua Street, 510640 Guangzhou, People's Republic of China

[‡]Institute of Geosciences, Kiel University, 24118 Kiel, Germany

[§]Institute for Energy and Climate Research (IEK-6), Forschungszentrum Jülich GmbH, 52428 Jülich, Germany

[⊥]Department of Civil Engineering and Geological Sciences and Department of Chemistry and Biochemistry, University of Notre Dame, 156 Fitzpatrick Hall, Notre Dame, Indiana 46556, United States

^{||}Actinide Chemistry Group, Chemical Sciences Division, Lawrence Berkeley National Laboratory, Berkeley, California 94720, United States

[¶]Department of Chemistry, University of California, Berkeley, Berkeley, California 94720, United States

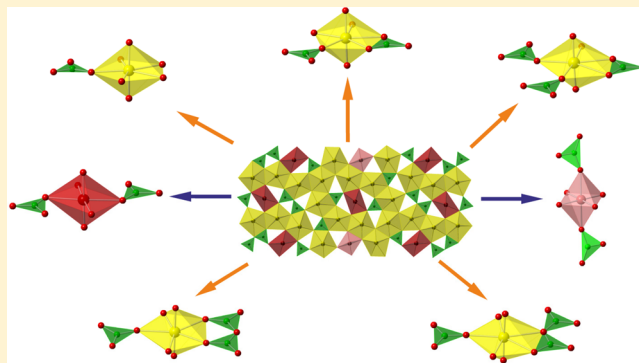
[▽]Mineralogisch-Petrographisches Institut, University of Hamburg, Grindelallee 48, 20146 Hamburg, Germany

[#]Department of Chemistry and Biochemistry, Florida State University, 102 Varsity Way, Tallahassee, Florida 32306-4390, United States

^{*}Institut für Kristallographie, RWTH Aachen University, 52066 Aachen, Germany

S Supporting Information

ABSTRACT: Three new potassium uranyl borates, $K_{12}[(UO_2)_{19}(UO_4)(B_2O_5)_2(BO_3)_6(BO_2OH)O_{10}] \cdot nH_2O$ (TPKBUO-1), $K_4[(UO_2)_5(BO_3)_2O_4] \cdot H_2O$ (TPKBUO-2), and $K_{15}[(UO_2)_{18}(BO_3)_7O_{15}]$ (TPKBUO-3), were synthesized under high-temperature/high-pressure conditions. In all three compounds, the U/B ratio exceeds 1. Boron exhibits BO_3 coordination only, which is different from other uranyl borates prepared at room temperature or under mild hydrothermal conditions. A rare uranium(VI) tetraoxide core UO_4O_2 , which is coordinated by two BO_3 groups, is observed in the structure of TPKBUO-1. Both structures of TPKBUO-1 and TPKBUO-3 contain three different coordination environments of uranium, namely, UO_4O_2 , UO_2O_4 , and UO_2O_5 and UO_2O_4 , UO_2O_5 , and UO_2O_6 bipyramids in TPKBUO-1 and TPKBUO-3, respectively.



1. INTRODUCTION

One nuclear waste management strategy includes vitrification of high-level radioactive waste in borosilicate glasses after reprocessing.¹ Although most of the uranium is being extracted from the waste during reprocessing, the produced borosilicate glasses contain some uranium and plutonium as well as neptunium² and up to 16.9% B_2O_3 .³ On the other hand, the Waste Isolation Pilot Plant (WIPP), located in New Mexico, is the world's only deep geologic repository for permanent storage of nuclear defense. The repository is located in the Salado Salt Formation, which is a high ionic strength salt brine comprised of several dissolved anionic components such as carbonate, sulfate, and borate, primarily in the form of H_3BO_3 , $B(OH)_4^-$, and $B_4O_7^{2-}$. The borate concentrations within the

salt brines can be as high as 166 ppm.⁴ In an effort to understand the solubility limiting phases that may be present upon closure of the repository, Borkowski et al. found that borate, not carbonate, is the primary complexant for trivalent actinide metals within the WIPP brines.⁵ While not a trivalent cation under repository conditions, there is a large amount of uranium, approximately 6.5×10^5 kg, stored at WIPP that is projected to be found as a 50/50 mixture of uranium(IV) and uranium(VI).⁴ As such, there exists the possibility that uranium(VI) and borate may come into contact and react

Received: January 3, 2013

Published: April 8, 2013

within the repository as decaying nuclear wastes, leading to heating beyond ambient temperatures.

Because of the large cross section and neutron-capture abilities of boron-10, enriched boric acid is generally used in nuclear reactors to absorb neutrons and as a corrosion inhibitor. This was certainly the case during the earthquake and subsequent tsunami that crippled the Fukushima Daiichi nuclear power plant. In an effort to prevent the nuclear fuel rods from melting down, large amounts of seawater and boric acid were pumped into the reactors.⁶ It is believed that the cladding of the fuel rods failed, thus exposing the hot fuel to concentrated boric acid. Because the fuel used in the reactors at Fukushima was mainly that of low enriched uranium, there exists the possibility that both uranium(IV) and uranium(VI) borates may have formed in this unfortunate event.

We have extended the knowledge of actinide borate chemistry significantly using boric acid as a reactive flux over the course of the past 3 years.^{7–9} Including the phases synthesized by Gasperin^{10–15} and Behm,¹⁶ there are at present 33 uranyl borates known. In all of these compounds, the molar ratio of uranium to boron is less than or equal to 1.^{7–16} Except for β - $\text{UO}_2\text{B}_2\text{O}_4$ (only BO_3 groups), boron exhibits both BO_3 and BO_4 coordination in all of the uranyl borates obtained by room temperature¹⁶ or boric acid flux methods.⁷ By way of contrast, the high-temperature phases reported by Gasperin^{10–15} are solely based on BO_3 units, with only one exception, $\text{Ni}_7\text{B}_4\text{UO}_{16}$, which contains both BO_3 and BO_4 .¹⁴ This lends itself to the statement that, as a rule, the coordination number of boron tends to be lower in high-temperature uranyl borates than in the low-temperature phases.

The influence of high-temperature/high-pressure (HT/HP) conditions on the formation of uranyl borate formation is underexplored. We have therefore started a systematic investigation of uranyl borate systems under HT/HP conditions and found that the reaction conditions are crucial for the formation and structures of uranyl borates. Herein, we report three new uranyl borates, which are synthesized using HT/HP methods, $\text{K}_{12}[(\text{UO}_2)_{19}(\text{UO}_4) - (\text{B}_2\text{O}_5)_2(\text{BO}_3)_6(\text{BO}_2\text{OH})_{10}] \cdot n\text{H}_2\text{O}$ (TPKBUO-1, HT/HP, potassium uranyl borate), $\text{K}_4[(\text{UO}_2)_5(\text{BO}_3)_2\text{O}_4] \cdot \text{H}_2\text{O}$ (TPKBUO-2), and $\text{K}_{15}[(\text{UO}_2)_{18}(\text{BO}_3)_7\text{O}_{15}]$ (TPKBUO-3). A significant feature of these structures is that the ratios of uranium to boron are higher than 1, with values of 1.81, 2.50, and 2.57 for TPKBUO-1, TPKBUO-2, and TPKBUO-3, respectively. Furthermore, all of the boron atoms adopt only 3-fold coordination (BO_3).

2. EXPERIMENTAL SECTION

2.1. Syntheses. $\text{UO}_2(\text{NO}_3)_2 \cdot 6\text{H}_2\text{O}$ (Merck), KNO_3 (Alfa-Aesar), H_3BO_3 (Alfa-Aesar), SiO_2 (amorphous), and α - Al_2O_3 (Alfa-Aesar) were used as received. All three uranyl borate phases were obtained during the study of systems relevant to nuclear glasses (borosilicate glasses or boroaluminum glasses). Therefore, SiO_2 and Al_2O_3 were used in the syntheses. The yield of all phases can not be calculated because of the presence of an amorphous product and the sticking of crystals on the wall of capsules especially for TPKBUO-3. The estimated yields should be between 10% and 30%. **Caution!** The $\text{UO}_2(\text{NO}_3)_2 \cdot 6\text{H}_2\text{O}$ used in this study contained depleted uranium; standard precautions for handling radioactive materials should be followed.

$\text{K}_{12}[(\text{UO}_2)_{19}(\text{UO}_4)(\text{B}_2\text{O}_5)_2(\text{BO}_3)_6(\text{BO}_2\text{OH})_{10}] \cdot n\text{H}_2\text{O}$ (TPKBUO-1). KNO_3 , H_3BO_3 , SiO_2 , α - Al_2O_3 , and $\text{UO}_2(\text{NO}_3)_2 \cdot 6\text{H}_2\text{O}$ (molar ratio K:B:Si:Al:U = 2:6:5:5:1) were ground together in an agate mortar. A total of 32.8 mg of the ground reactants and 10 μL of KOH (1 M) were sealed in a gold capsule. The synthesis was performed at $T = 650$

± 5 °C and $P = 200 \pm 10$ MPa for 7 days in a cold-seal pressure vessel containing H_2O as the pressure medium. The details of the synthesis were similar to those reported in a previous study.¹⁵ Yellow prismatic crystalline products of TPKBUO-1 were obtained with crystal quality suitable for a single-crystal X-ray diffraction study. The remaining material was a white amorphous product (probably containing SiO_2 and Al_2O_3). In other syntheses [e.g., K:B:Al:U = 2:6:5:1, 7 μL of KOH (1 M)], TPKBUO-1 was always obtained together with the known $\text{UO}_2[\text{B}_3\text{Al}_4\text{O}_{11}(\text{OH})]$.¹⁷ TPKBUO-1 (yellow) was easily identified from $\text{UO}_2[\text{B}_3\text{Al}_4\text{O}_{11}(\text{OH})]$ (green) because of the different colors of the crystals.

$\text{K}_4[(\text{UO}_2)_5(\text{BO}_3)_2\text{O}_4] \cdot \text{H}_2\text{O}$ (TPKBUO-2). A total of 32.1 mg of a ground mixture of KNO_3 , H_3BO_3 , SiO_2 , and $\text{UO}_2(\text{NO}_3)_2 \cdot 6\text{H}_2\text{O}$ (molar ratio K:B:Si:U = 2:6:5:1) was sealed in a gold capsule. The synthesis temperature, pressure, and other experimental parameters were the same as those for TPKBUO-1, with the exception that neither Al_2O_3 nor KOH was used. Yellow tablet crystals of TPKBUO-2 were isolated from an amorphous phase and used for crystallographic studies.

$\text{K}_{15}[(\text{UO}_2)_{18}(\text{BO}_3)_7\text{O}_{15}]$ (TPKBUO-3). In a typical synthesis, KNO_3 , H_3BO_3 , SiO_2 , and $\text{UO}_2(\text{NO}_3)_2 \cdot 6\text{H}_2\text{O}$ (molar ratio K:B:Si:U = 2:6:5:1) were ground and a mixture of 46.4 mg was placed in a platinum capsule (outer diameter = 4.4 mm, inner diameter = 4 mm, and length = 8 mm). The capsule was sealed and inserted into the center of a 6-mm-diameter MgO spacer. The MgO spacer was positioned at the center of a tapered graphite furnace. The graphite furnace was contained in sleeves of pyrex glass and a pyrophyllite pressure medium. The experiment was performed at a pressure of 2.5 GPa and in the temperature range from 1200 to 700 °C using the $1/2$ -in. piston cylinder module of a Vöggenreiter LP 1000-540/50. The experiment was performed with the “cold piston” method: all piston cylinder assemblies were pressurized cold to about 90% of the desired pressure within 10 min. The temperature was then raised to 1200 °C with a heating rate of 100 °C/min, while the pressure was kept constant. After the final temperature of 1200 °C was reached, the assembly was pressurized to the final pressure of 2.5 GPa. Temperature and pressure were automatically controlled during the experiment. While the pressure was kept constant at 2.5 GPa during the experiment, the temperature remained at 1200 °C only for 60 min. After that, the sample was cooled to 700 °C at a rate of 7 °C/h. Finally the sample was quenched to room temperature by turning off the power to the graphite heater, and the pressure was released within 10 min. Yellow tablet crystals of TPKBUO-3 together with yellow prismatic crystals of uranyl silicate (which will be reported elsewhere) were obtained. More details on the experimental procedure may be found in our previous work.¹⁸

2.2. Crystallographic Studies. Crystals selected for data collection were mounted on a Nonius CCD four-circle diffractometer. All data were collected using monochromatic Mo $K\alpha$ radiation ($\lambda = 0.71073$ Å). The unit-cell dimensions for all compounds (Table 1) were refined by least-squares techniques against the positions of all measured reflections. More than one hemisphere of data was collected for each crystal. The three-dimensional (3D) data were integrated and corrected for Lorentz, polarization, and background effects using the Eval14 procedures,¹⁹ as implemented in the supporting programs for the diffractometer. Data were scaled and corrected for absorption effects using SADABS. Additional information pertinent to the data collection is given in Table 1. The SHELXL-97 program²⁰ was used for the determination and refinement of the structures. The structures were solved by direct methods and refined to $R_1 = 0.0333$ for TPKBUO-1, 0.0376 for TPKBUO-2, and 0.0640 for TPKBUO-3.

The yield and quality of the crystals of TPKBUO-3 were quite low. Consequently, the quality of the diffraction data is significantly lower than that from TPKBUO-1 and TPKBUO-2. However, the model obtained from the refinement is reasonable and justifies including this information in this paper because of its importance for comparison with the other uranyl borates synthesized from HT/HP conditions. The low crystal quality might result from pressure quenching and may indicate phase instability at normal pressure.

Table 1. Crystallographic Data for TPKBUO-1, TPKBUO-2, and TPKBUO-3

	TPKBUO-1	TPKBUO-2	TPKBUO-3
color and habit	yellow, prism	yellow, tablet	yellow, tablet
cryst syst	orthorhombic	monoclinic	monoclinic
space group	<i>Pmcb</i>	<i>P2₁/c</i>	<i>P2₁/m</i>
<i>a</i> (Å)	6.9284(4)	6.801(6)	13.438(7)
<i>b</i> (Å)	13.3816(16)	11.831(10)	6.850(4)
<i>c</i> (Å)	49.865(4)	13.330(12)	22.238(12)
α (deg)	90	90	90
β (deg)	90	90.207(10)	107.586(13)
γ (deg)	90	90	90
<i>V</i> (Å ³)	4623.1(7)	1072.4(16)	1951.3(18)
<i>Z</i>	1	2	1
<i>T</i> (K)	293	293	293
λ (Å)	0.71073	0.71073	0.71073
reflns collected	92095	11601	22221
indep reflns	5314	2275	4497
indep reflns with $I > 2\sigma(I)$	4359	1961	1894
max 2θ (deg)	53.46	57.04	53.44
ρ_{calcd} (g/cm ³)	4.906	5.277	5.190
μ (Mo <i>K</i> α) (cm ⁻¹)	355.47	384.85	381.03
$R(F)$ for $F_o^2 > 2\sigma(F_o^2)^a$	0.0333	0.0376	0.0640
$R_w(F_o^2)^b$	0.0680	0.0920	0.1849

$$^a R(F) = \sum ||F_o| - |F_c|| / \sum |F_o|. \quad ^b R(F_o^2) = [w(F_o^2 - F_c^2)^2 / \sum w(F_o^4)]^{1/2}.$$

2.3. IR Spectroscopy. IR spectra were obtained from single crystals using a SensIR technology IlluminatIR Fourier transform infrared (FT-IR) microspectrometer. A single crystal was placed on a glass slide, and the spectrum was collected with a diamond ATR objective. Each spectrum was scanned from 650 to 4000 cm⁻¹ with a beam aperture of 100 μ m.

2.4. UV–Vis–Near-IR (NIR) Spectroscopy. UV–vis–NIR spectra data were obtained from single crystals using a Craic Technologies UV–vis–NIR microspectrophotometer. Crystals were placed on quartz slides under Krytox oil, and the data were collected from 500 to 1400 nm.

3. RESULTS AND DISCUSSION

3.1. Syntheses and Chemical Compositions. All three phases were obtained from HT/HP reactions. The synthesis temperature and pressure were the same for TPKBUO-1 and TPKBUO-2, with the only difference being the presence of Al₂O₃ and KOH as starting materials in the experiment yielding TPKBUO-1. The pH of the system probably controls the formation of different phases. As mentioned in section 2.1, when less KOH was used, both TPKBUO-1 and another known phase, UO₂[B₃Al₄O₁₁(OH)], formed. In the absence of KOH, TPKBUO-1 was observed. Although aluminum and silicon are not incorporated into the structures, Al₂O₃ and SiO₂ used in the experiments might be inducers for different phases. For example, during the synthesis of TPKBUO-2, when SiO₂ was absent, a mixture of TPKBUO-2 and known structure (UO₂[B₃Al₄O₁₁(OH)])¹⁷ was observed. However, TPKBUO-2 was yielded as a single uranium-containing phase when SiO₂ was present. On the other hand, TPKBUO-2 and TPKBUO-3 were obtained from the same starting materials but at different pressures and temperatures. It is well-known that both the pressure and temperature are important parameters for the formation of different phases.²¹ Because both the pressure and temperature are different in the synthesis of TPKBUO-2 and TPKBUO-3, it is impossible to conclude which parameter is dominated. More investigations are required to figure out the

phase equilibrium of TPKBUO-2, TPKBUO-3, and other possible phases.

As we have noted before, the U/B ratios are 1.81, 2.50, and 2.57 in TPKBUO-1, TPKBUO-2, and TPKBUO-3, respectively. In all three phases, boron is 3-fold-coordinated (BO₃). This kind of coordination environment is the same as that for most of the phases obtained by high-temperature solid-state reactions of Gasperin,^{10–13,15} except for Ni₇B₄UO₁₆, where both BO₃ and BO₄ exist.¹⁴ With the exception of β -UO₂B₂O₄ (only BO₃ groups), both BO₃ triangles and BO₄ tetrahedra were observed in all uranyl borate phases synthesized at room temperature and from boric acid flux reactions.^{7,9,16} This implies that, in the uranyl borate systems, boron lowers its coordination number with increasing temperature. Considering the effect of pressure on the coordination of boron, Werdning and Schreyer studied several systems in the pressure range from 3 to 5 GPa.²² Most of the isolated borates were BO₃, except it was in the position of silicon or aluminum where it adopted a coordination number of 4.²² In Huppertz's investigations, higher pressures up to 10.5 GPa were used and more complicated structures were observed.²³ For example, in the system of Dy₂O₃–B₂O₃, boron increased its coordination number from BO₃ in ν -DyBO₃²⁴ to mixed BO₃ and BO₄ in β -Dy₂B₄O₉,²⁵ and only BO₄ in α -Dy₂B₄O₉²⁶ with increasing pressure from 3 GPa (1050 °C) to 8 GPa (1000 °C) and 10 GPa (1150 °C), respectively. In the present study, the used temperatures and pressures were 650 °C/200 MPa and 1200 °C/2.5 GPa, and boron showed only 3-fold coordination. Comparably, in the structure of β -HgB₄O₇, which was synthesized at 600 °C/7.5 GPa, only BO₄ was observed.²⁷ This probably indicates that the pressure is dominated compared to the temperature at HT/HP conditions.

3.2. Crystal Structures. In oxo compounds, uranium(VI) usually forms nearly linear UO₂²⁺ uranyl units that form strong, short, and generally unreactive U–O bonds. Additional oxygen atoms can bond in the equatorial plane perpendicular to the UO₂²⁺ groups, thus forming quadratic, pentagonal, or hexagonal bipyramids as typical coordination polyhedra. The equatorial bonds are considerably weaker than the bonds within the uranyl group and tend to polymerize the bipyramids or join with other oxoanions, such as borate groups. This anisotropic bonding character results in the frequently observed layer-like character of uranyl compounds in general and in the title compounds in particular. The layer-to-layer distance in the title compounds is on the order of 3.5 Å, giving a lattice parameter of slightly less than 7 Å (lattice parameter *a* in TPKBUO-1 and TPKBUO-2 but *b* in TPKBUO-3). The layers of the three compounds are composed of various bipyramids and borate groups but have a common unit-cell dimension of about 13.5 Å. This is roughly the length of the zigzag chains of four UO₂O₅ pentagonal bipyramids running in different directions of the three compounds. The second intralayer dimension is quite different for the three compounds and varies from about 12 Å (TPKBUO-2) to 22 Å (TPKBUO-3) to 50 Å (TPKBUO-1) because of the different arrangements of the various oxouranium polyhedra and borate groups.

TPKBUO-1. The layers of TPKBUO-1 are connected by BO₃ groups, resulting in a complex 3D framework (Figure 1a). The layers are parallel to the *bc* plane and are based on a variety of oxouranium and oxoboron units (Figure 1b). The structure of TPKBUO-1 is the fourth example of uranium(VI) inorganic compounds (including two minerals, phosphuranylite and vanmeerscheite) where uranium atoms have three different

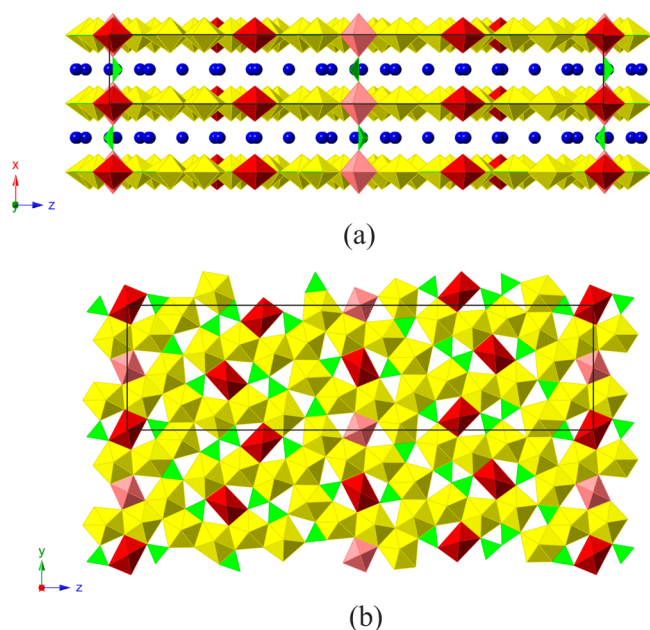


Figure 1. View of the structure of **TPKBUO-1**. UO_2O_4 square bipyramids are shown in red, UO_2O_5 pentagonal bipyramids are shown in yellow, UO_4O_2 [uranium(VI)] tetraoxo cores are shown in pink, BO_3 units are shown in green, and K^+ cations are shown in blue.

types of coordination environments.²⁸ One of them is a square bipyramid UO_2O_4 , while the second one is a pentagonal bipyramid UO_2O_5 (shown in red and yellow in Figure 1, respectively). The U–O bond lengths within these polyhedra range from 1.78(1) to 1.81(1) Å for the axial uranyl groups (UO_2^{2+}) and from 2.19(1) to 2.75(1) Å for the equatorial bonds. The third uranium coordination (shown in pink in Figure 1) is rather rare and is known as a tetraoxo core.^{29–32} In this case, uranium atoms have UO_4O_2 coordination, where four short equatorial U–O bonds are similar [$2 \times 1.95(1)$ Å and $2 \times 2.07(1)$ Å] and two axial bonds are significantly enlarged [$2.20(3)$ Å] compared to “normal” U–O distances. Both types of UO_2O_4 and UO_2O_5 are linked to oxoborate groups in their equatorial planes. **TPKBUO-1** contains BO_3 monomers and B_2O_5 dimers within the layers. The B–O bond lengths are within the range of 1.30(3)–1.42(2) Å. Additional BO_3 groups span the interlayer space, thus providing linkage of the uranium borate layers to form a 3D framework (Figure 1a). These groups share oxygen atoms with the UO_4O_2 polyhedra. This BO_3 group is quite distorted, and according to bond valence sum analysis,³³ it most probably contains a protonated terminal oxygen atom (O33) directed into the interlayer space. Thus, BO_2OH groups provide linkage of the layers into the 3D framework. The B–O bond lengths within the discussed BO_3 group range from 1.33(3) to 1.53(16) Å.

The potassium atoms reside between the layers and compensate for the negative charge of the framework. The relief of the layer surface is quite rough, and this might be the reason why some potassium positions are disordered. The rest of the free interlayer space in **TPKBUO-1** is occupied by disordered H_2O molecules, the presence of which has been confirmed by the IR spectrum at around 1600 cm^{-1} (Figure 7). The number of disordered H_2O is undetermined and, therefore, n was used in the formula.

TPKBUO-2. The layers of **TPKBUO-2** extend parallel to the $[bc]$ plane (Figure 2). The structure of this phase is less

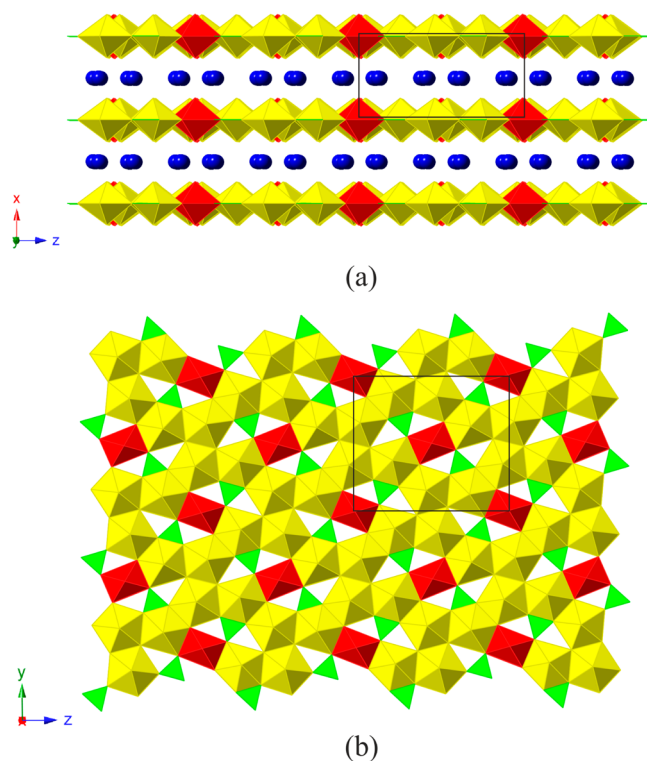


Figure 2. View of the structure of **TPKBUO-2**. UO_2O_4 square bipyramids are shown in red, UO_2O_5 pentagonal bipyramids are shown in yellow, BO_3 units are shown in green and K^+ cations are shown in blue.

complex than those of the other two compounds described. The coordination of uranium is represented by two sorts of polyhedra, viz. UO_2O_4 square bipyramids and UO_2O_5 pentagonal bipyramids (Figure 2, shown in red or yellow, respectively). The bond lengths within the uranyl groups range from 1.79(1) to 1.81(1) Å. The bond angle in the uranyl group range from $178.8(5)^\circ$ to $179.0(5)^\circ$ within a pentagonal bipyramidal, whereas it is 180° within the square bipyramids resulting from the special position of U2. The equatorial bonds within the polyhedra are in the range of 2.18(9) Å (for UO_2O_4) to 2.45(1) Å (for UO_2O_5). The layers in **TPKBUO-2** possess only one type of monomeric oxo-borate group (BO_3 , shown in green in Figure 2), in contrast to **TPKBUO-1** where monomeric and dimeric groups are present. The bond lengths in BO_3 groups are in the range of 1.34(2) to 1.37(2) Å while the borate bond angles are very close to the ideal value of 120° .

In contrast to **TPKBUO-1** and **TPKBUO-3**, the K^+ cation sites and H_2O molecules residing in the interlayer space in **TPKBUO-2** are fully occupied. This may be the result of the relatively low complexity of the layers in the structure of **TPKBUO-2**.

TPKBUO-3. The layers of **TPKBUO-3** consist of three different uranium coordination polyhedra and BO_3 groups (Figure 3). All uranium atoms form linear uranyl groups (UO_2^{2+}) and have four (UO_2O_4 , shown in red in Figure 3), five (UO_2O_5 , yellow in Figure 3), or six (UO_2O_6 , orange in Figure 3) atoms in the equatorial plane. The structure of **TPKBUO-3** is the fourth known uranyl phase containing three different equatorial coordinations and the fifth (including **TPKBUO-1**) uranium compound with three different uranium(VI) environments present within a single phase. The U–O bond lengths within the uranium polyhedra range from 1.77(2) to 1.82(3) Å

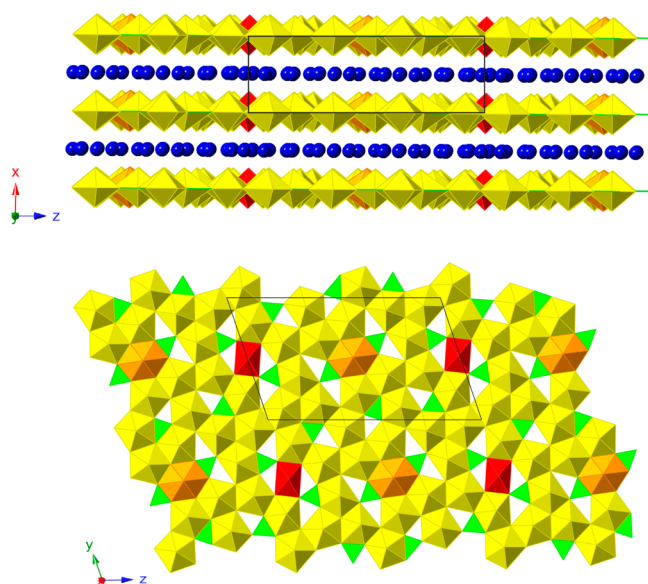


Figure 3. View of the structure of TPKBUO-3. The BO_3 group around $(x, 0, 1/2)$ is statistically disordered. For the sake of clarity, only one position is shown, but the disorder is indicated by showing either orientation at translationally equivalent positions, e.g., at $(x, 0, 1/2)$ and $(x, -1, 1/2)$ or $(x, 0, -1/2)$. UO_2O_4 square bipyramids are shown in red, UO_2O_5 pentagonal bipyramids are shown in yellow, UO_2O_6 hexagonal bipyramids are shown in orange, BO_3 units are shown in green, and K^+ cations are shown in blue.

for uranyl groups and from 2.15(2) to 2.79(2) Å for the equatorial bonds. The geometry of the BO_3 groups is quite distorted, which is a consequence of low crystal quality. The B–O bond lengths are in the range from 1.27(9) to 1.58(8) Å, resulting in O–B–O angles ranging from 94(5)° to 144(4)°.

The positions of the potassium atoms within the interlayer space are partially disordered. This might be a result of the complex form of the free volume between layers similar to that observed in TPKBUO-1 and/or rapid quenching from high pressure.

Local Configurations of Uranium. The structural complexity of the layers in these phases add to our knowledge of the diversity of the uranium coordination chemistry. For comparison, the uranium atoms in the structures of uranyl borates obtained by low-temperature H_3BO_3 flux reactions exhibit only two different patterns of borate environments^{5,7} with either six or nine borate groups but a variable number of BO_3 triangles and BO_4 tetrahedra. In variance with the phases obtained by H_3BO_3 flux reactions, the title compounds contain significantly less boron. Because the uranium polyhedra are not completely surrounded by oxygen donors from borate units, a wider range of the geometries about the uranium centers is possible. The various geometries found in the structures of TPKBUO-1, TPKBUO-2, and TPKBUO-3 are shown in Figure 4. In total, there are 10 different geometries, where the simplest one is based on a single pentagonal bipyramid and a BO_3 triangle (Figure 4a). Such clusters are found in the structures of TPKBUO-1 and TPKBUO-3 but are absent in TPKBUO-2.

Clusters based on three groups (one uranyl polyhedron and two borate triangles) occur in six different configurations (Figure 4b–d,h–j). Only two of them (b and h) are present in all three structures. The geometry d is present in TPKBUO-2 and TPKBUO-3, but the remaining ones are present in only

one phase, viz., c and i in TPKBUO-1 and j in TPKBUO-3. The cluster type shown in Figure 4i is quite similar to that observed in the structure of $\text{Ba}_4[(\text{UO}_2)_7(\text{UO}_4)(\text{AsO}_4)_2\text{O}_7]$ but has flat BO_3 triangles instead of AsO_4 tetrahedra capping the uranium polyhedron.²⁰ The coordination shown in Figure 4j is closely related to the one found in some uranium carbonate minerals, such as fontanite.³⁴

There are three geometrical types based on three BO_3 triangles and a single uranyl group (Figure 4e–g). All of them include BO_3 as well as B_2O_5 groups and are found in the structure of TPKBUO-1. These configurations have not been observed before in any other inorganic uranium compound.

3.3. Topological Complexity. All investigated phases possess topological features that are new for the family of oxouranium phases. TPKBUO-1 and TPKBUO-3 exhibit extreme topological complexity as a consequence of their chemical composition and the diversity of uranium borate clusters described above. To describe the topological diversity, we employ the anion topology method developed by Burns et al.³⁵ TPKBUO-2 has the simplest topology of its layers. P chains (based on edge-sharing pentagons, shown in dark gray in Figure 5) combine with modified R chains (with added triangular units, denoted here as R_T chains, shown in gray and green in Figure 5) and form the topology shown in Figure 5. This topology can be described as a complication of the sayrite topology with the addition of triangular units and can be described as $\dots\text{PR}_T\text{PR}_T\text{PR}_T\text{P}\dots$ ³⁶

The topology of layers in TPKBUO-3 is shown in Figure 6a. It is possible to separate out PR_TP fragments within the layers consisting of two P and one R_T chains. Between them, one can see a hexagon surrounded by four pentagons and two triangles (two such clusters are emphasized by the orange color). Such clusters are commonly found for uranyl carbonates where they form infinite one-dimensional (1D) chains.^{34,37} However, in the layers of TPKBUO-3, they are not linked with each other but separated by pentagonal dimers and triangle fragments. Thus, the topology of TPKBUO-3 is based on fragments observed in TPKBUO-2 and modified uranyl-carbonate-like units.

The topology of TPKBUO-1 is unprecedented in uranium crystal chemistry. Three main building units can be distinguished in the layers of TPKBUO-1, viz., pentagons, quadrangles, and triangles (Figure 6b). There is no obvious way to separate out a periodic 1D structure with reasonable complexity in TPKBUO-1. One can, however, separate out an agglomerate of 16 edge-sharing pentagons (shown in yellow in Figure 6b). The very long c parameter (~ 49 Å) in TPKBUO-1 results from the presence of such large fragments. These fragments are packed within the layers in a sawtooth-like mode. They are linked by quadrangular and triangular groups to form the periodic 2D structure.

3.4. Spectroscopic Properties. In the IR spectra shown in Figure 7, the peaks at 1610 and 1620 cm^{-1} are assigned to δ H_2O (bending vibration), which confirms the presence of H_2O in the structures of TPKBUO-1 and TPKBUO-2. Meanwhile, the peaks at 3536–3580 and 3468 cm^{-1} indicate the hydroxyl groups in the structures of TPKBUO-1 and TPKBUO-2 (Figure 7, inset). In the spectrum of TPKBUO-3, the absence of bands at around 1600 and 3500 cm^{-1} demonstrated the absence of H_2O and hydroxyl groups in the structure of TPKBUO-3. Bands between 1100 and 1400 cm^{-1} can be assigned to the antisymmetric stretching vibrations (ν_3) of the BO_3 groups.³⁸ The bands at 650–850 and 850–1000 cm^{-1} are

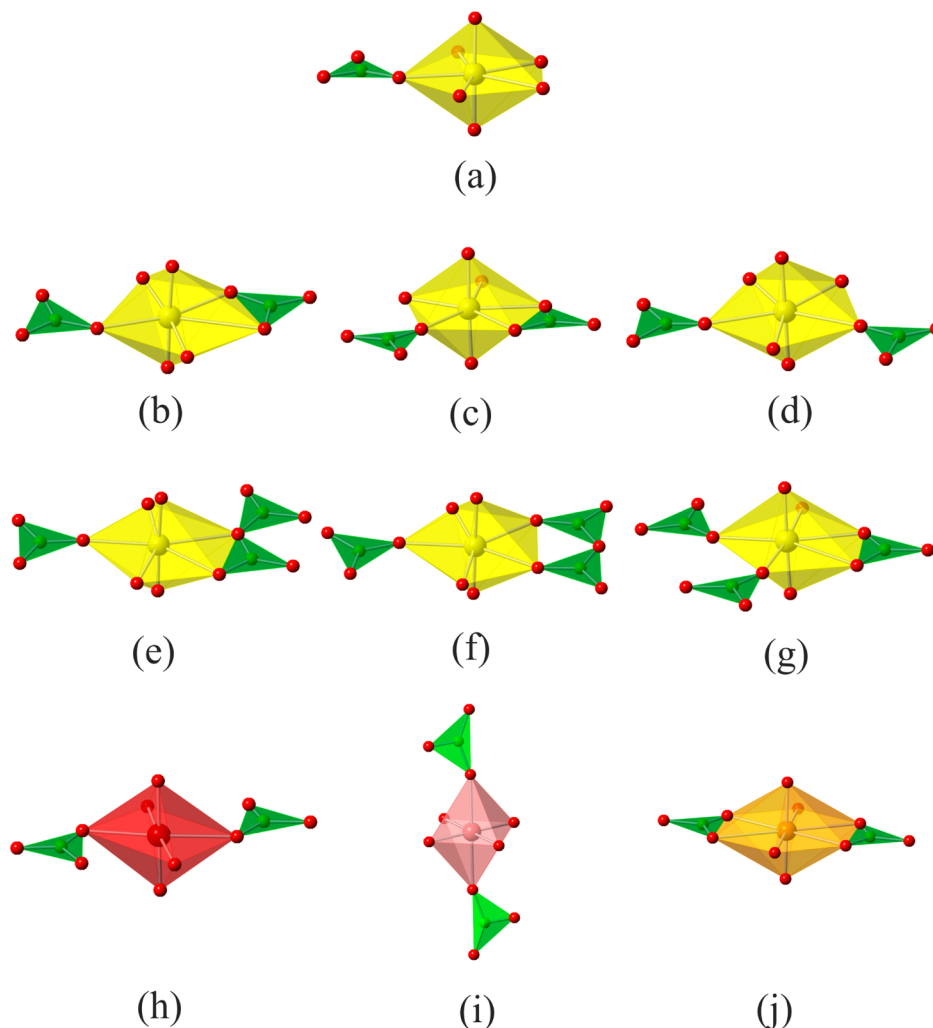


Figure 4. Different geometries of $(\text{UO}_2)^{2+}$ and $(\text{UO}_4)^{2-}$ centers with BO_3 groups (shown in green) in **TPKBUO-1**, **TPKBUO-2**, and **TPKBUO-3**.

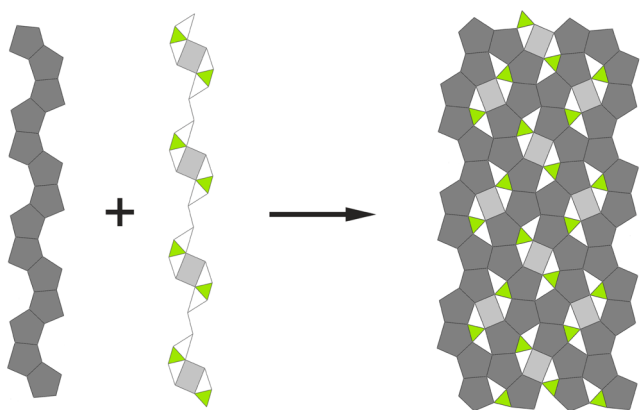


Figure 5. Anion topology observed in **TPKBUO-2**. UO_2O_5 pentagons are shown in dark gray, UO_2O_4 square bipyramids are shown in gray, and BO_3 units are shown in green.

attributed to the ν_3 (UO_2)²⁺ and ν_1 (symmetric stretching vibrations) (UO_2)²⁺.³⁹ It is noteworthy that there may also be some coincidences with ν_1 and ν_3 of the BO_3 group in the range between 650 and 1000 cm^{-1} .³⁸ In the case of **TPKBUO-1**, the band at 1406 cm^{-1} is probably due to the contribution of the B_2O_5 unit.⁴⁰ Theoretically, there should be some bands attributed to the UO_4 group in **TPKBUO-1**. However, it is

difficult to distinguish the contributions of UO_4 and $(\text{UO}_2)^{2+}$ whether in this study or in Weng et al.'s work.³²

$(\text{UO}_2)^{2+}$ in both the solid state and solution produces a vibrationally coupled electronic transition around 420 nm, which is attributed to a singlet–triplet transition between the highest occupied and lowest unoccupied molecular orbitals of $(\text{UO}_2)^{2+}$ derived by hybridization of uranium 5f and oxygen 2p orbitals.⁴¹ The solid-state UV–vis–NIR spectra of **TPKBUO-1**, **TPKBUO-2**, and **TPKBUO-3** are shown in Figure 8. **TPKBUO-1** containing both a linear dioxo (UO_2)²⁺ unit and a tetraoxido core (UO_4)²⁻ unit exhibits a strong peak at ~350 nm and a transition at ~430 nm, which is typical for uranium(VI) compounds such as $\text{UO}_2(\text{NO}_3)_2 \cdot 6\text{H}_2\text{O}$.³² Notably, the spectrum of **TPKBUO-1** is very similar to that observed for **TPKBUO-2**, which contains only $(\text{UO}_2)^{2+}$ units. Recently, Burns et al. reported a uranium(VI) compound containing both $(\text{UO}_2)^{2+}$ and $(\text{UO}_4)^{2-}$, $(\text{UO}_2)_2[\text{UO}_4(\text{trz})_2](\text{OH})_2$ (trz = 1,2,4-triazole), which also shows a similar spectrum.³² In contrast, the first reported uranium(VI) compound containing $(\text{UO}_4)^{2-}$, $\text{Cd}_2(\text{H}_2\text{O})_2[\text{U}(\text{OH})(\text{CH}_3\text{COO})(\text{UO}_2)_5(\text{OH})_2\text{O}_8] \cdot 0.5\text{H}_2\text{O}$, produces a single broad feature around 420 nm, which is similar to the cation–cation interaction of a uranium(VI) compound³² and aqueous $(\text{UO}_2)^{2+}$.⁴² This implies that the contribution of the uranium(VI) tetraoxido core might be coincident with

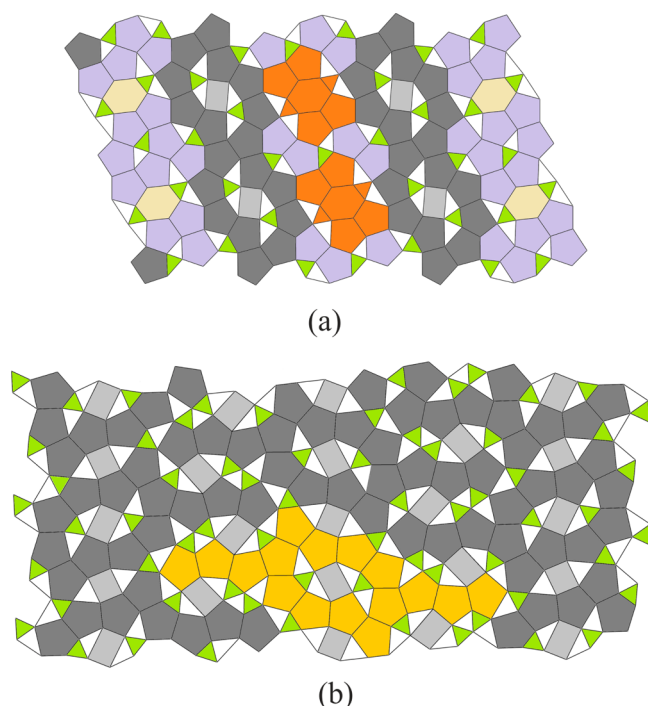


Figure 6. Anion topology observed in the structures of TPKBUO-3 (a) and TPKBUO-1 (b). UO_2O_6 hexagonal bipyramids are shown in pale yellow, UO_2O_5 pentagons are shown in dark gray and purple, UO_2O_4 square bipyramids are shown in gray, and BO_3 units are shown in green. The hexagonal bipyramid surrounding environment is emphasized in orange in part a, and the agglomerate of 16 edge-sharing pentagons is shown in yellow in part b.

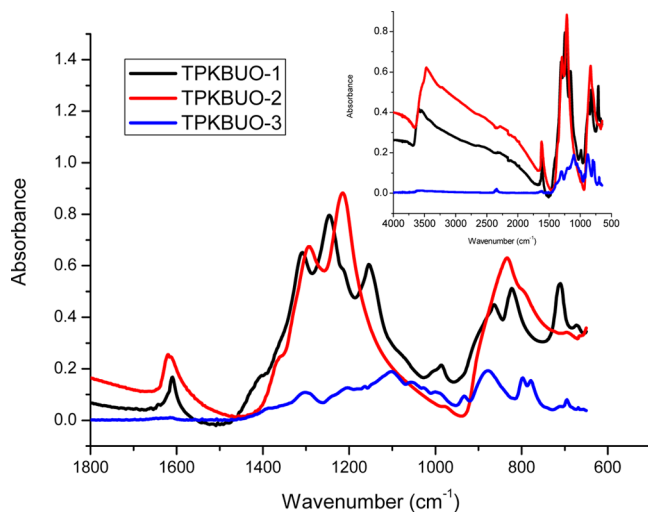


Figure 7. FT-IR spectra of TPKBUO-1, TPKBUO-2, and TPKBUO-3.

$(\text{UO}_2)^{2+}$ in UV-vis-NIR spectra or there is no special contribution.

The solid-state fluorescence spectra of all phases are quiet weak; therefore, the data are not shown. The reason is not clear right now, but it is probably due to the special coordination of the borate group with the uranyl ion, which quenches the fluorescence in these structures. It is interesting that all of the potassium uranyl borates with U/B less than or equal to 1 possess strong fluorescence.^{7a,43} Contrarily, the UV-vis-NIR

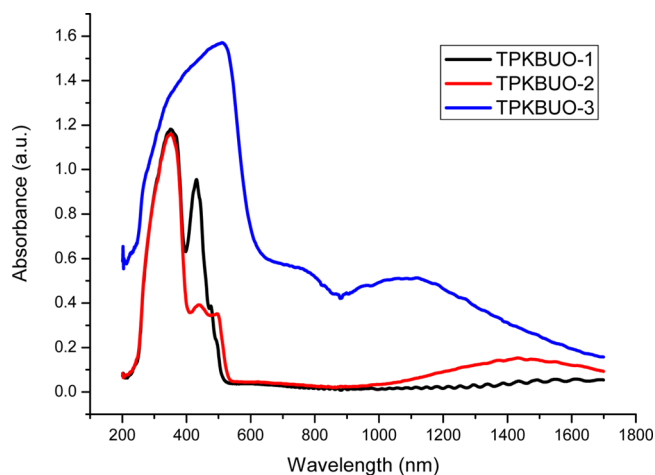


Figure 8. UV-vis-NIR spectra of TPKBUO-1, TPKBUO-2, and TPKBUO-3.

spectra are similar especially for TPKBUO-1, TPKBUO-2, and $\text{K}(\text{UO}_2)(\text{BO}_3)$.⁴³

4. CONCLUSIONS

In conclusion, we have synthesized three new potassium uranyl borates, TPKBUO-1, TPKBUO-2, and TPKBUO-3, using high-temperature (at 650 and 1200 °C) and high-pressure (at 200 and 2.5 GPa) methods. The structures of TPKBUO-2 and TPKBUO-3 are typical layered structures, while in TPKBUO-1, layers are connected by BO_3 groups to form a 3D framework structure. In all three structures, boron adopts BO_3 coordination and the U/B ratio is higher than 1. This is different from most of the other uranyl borates known up to date. In addition, the structure of TPKBUO-1 contains the rare uranium(VI) tetraoxide core (UO_4O_2). The structures of TPKBUO-1 and TPKBUO-3 represent new examples of structures with three different coordination environments of uranium(VI). Finally, our work shows that the HT/HP chemistry of the $\text{A}^+-\text{UO}_3-\text{B}_2\text{O}_3$ system (A^+ = alkali elements) is markedly different from that at low pressures with respect to both the chemical composition of the reaction products and their structural features.

■ ASSOCIATED CONTENT

Supporting Information

CIF files for TPKBUO-1, TPKBUO-2, and TPKBUO-3. This material is available free of charge via the Internet at <http://pubs.acs.org>.

■ AUTHOR INFORMATION

Corresponding Author

*E-mail: albrecht-schmitt@chem.fsu.edu (T.E.A.-S.), alekseev@fz-juelich.de (E.V.A.).

Author Contributions

All authors have given approval to the final version of the manuscript.

Notes

The authors declare no competing financial interest.

■ ACKNOWLEDGMENTS

We are grateful for the support provided by Deutsche Forschungsgemeinschaft (Grant DE 412/43-1) and by the

Chemical Sciences, Geosciences, and Biosciences Division, Office of Basic Energy Sciences, Office of Science, Heavy Elements Chemistry Program, U.S. Department of Energy (Grant DE-FG02-09ER16026), Helmholtz Association (Grant VH-NG-815), and National Natural Sciences Foundation of China (Grant 41103055).

REFERENCES

- (1) (a) Commission on Geosciences, Environment and Resources. *Glass as a waste form and vitrification technology: Summary of an international workshop*; National Academy of Science: Washington, DC, 1996. (b) International Atomic Energy Agency. *Spent fuel and high level waste: Chemical durability and performance under simulated repository conditions*; International Atomic Energy Agency: Vienna, Austria, 2007.
- (2) Grambow, B. *Elements* **2006**, *2*, 357–364.
- (3) Ojovan, M. I.; Batyukhnova, O. G. Glasses for nuclear waste immobilization. *Proceedings of WM'07*, Feb 27–Mar 1, 2007, Tuscon, AZ, 2007; Paper WM-7061.
- (4) United States Department of Energy. Waste Isolation Pilot Plant, Title 40 CFR Part 191 Subparts B and C Compliance Recertification Application for the Waste Isolation Pilot Plant. Appendix SOTERM-2009. Actinide Chemistry Source Term, Carlsbad, NM, 2009; DOE/WIPP-09-3424.
- (5) Borkowski, M.; Richmann, M.; Reed, D. T.; Xiong, Y. *Radiochim. Acta* **2010**, *98*, 577–582.
- (6) International Atomic Energy Agency. IAEA Fukushima Daiichi Status Report, Nov 2, 2011.
- (7) (a) Wang, S.; Alekseev, E. V.; Stritzinger, J. T.; Depmeier, W.; Albrecht-Schmitt, T. E. *Inorg. Chem.* **2010**, *49* (14), 6690–6696. (b) Wang, S.; Alekseev, E. V.; Ling, J.; Liu, G. K.; Depmeier, W.; Albrecht-Schmitt, T. E. *Chem. Mater.* **2010**, *22* (6), 2155–2163. (c) Wang, S.; Alekseev, E. V.; Stritzinger, J. T.; Liu, G. K.; Depmeier, W.; Albrecht-Schmitt, T. E. *Chem. Mater.* **2010**, *22* (21), 5983–5991. (d) Wang, S.; Alekseev, E. V.; Juan, D. W.; Miller, H. M.; Oliver, A. G.; Liu, G. K.; Depmeier, W.; Albrecht-Schmitt, T. E. *Chem. Mater.* **2011**, *23* (11), 2931–2939. (e) Wang, S.; Villa, E. M.; Diwu, J. A.; Alekseev, E. V.; Depmeier, W.; Albrecht-Schmitt, T. E. *Inorg. Chem.* **2011**, *50* (6), 2527–2533. (f) Wang, S.; Alekseev, E. V.; Depmeier, W.; Albrecht-Schmitt, T. E. *Chem. Commun.* **2011**, *47* (39), 10874–10885. (g) Wang, S.; Alekseev, E. V.; Miller, H. M.; Depmeier, W.; Albrecht-Schmitt, T. E. *Inorg. Chem.* **2010**, *49* (21), 9755–9757.
- (8) (a) Wang, S.; Alekseev, E. V.; Depmeier, W.; Albrecht-Schmitt, T. E. *Chem. Commun.* **2010**, *46* (22), 3955–3957. (b) Wang, S.; Alekseev, E. V.; Juan, D. W.; Casey, W. H.; Phillips, B. L.; Depmeier, W.; Albrecht-Schmitt, T. E. *Angew. Chem., Int. Ed.* **2010**, *49* (6), 1057–1060. (c) Wang, S.; Alekseev, E. V.; Ling, J.; Skanthakumar, S.; Soderholm, L.; Depmeier, W.; Albrecht-Schmitt, T. E. *Angew. Chem., Int. Ed.* **2010**, *49* (7), 1263–1266. (d) Wang, S.; Alekseev, E. V.; Depmeier, W.; Albrecht-Schmitt, T. E. *Inorg. Chem.* **2011**, *50* (11), 4692–4694. (e) Wang, S.; Alekseev, E. V.; Depmeier, W.; Albrecht-Schmitt, T. E. *Inorg. Chem.* **2011**, *50* (6), 2079–2081. (f) Polinski, M. J.; Wang, S.; Alekseev, E. V.; Depmeier, W.; Albrecht-Schmitt, T. E. *Angew. Chem., Int. Ed.* **2011**, *50* (38), 8891–8894. (g) Wang, S.; Diwu, J.; Alekseev, E. V.; Jouffret, L. J.; Depmeier, W.; Albrecht-Schmitt, T. E. *Inorg. Chem.* **2012**, *51* (13), 7013–7016. (h) Wang, S.; Alekseev, E. V.; Depmeier, W.; Albrecht-Schmitt, T. E. *Inorg. Chem.* **2012**, *51* (1), 7–9. (i) Polinski, M. J.; Wang, S.; Alekseev, E. V.; Depmeier, W.; Liu, G.; Haire, R. G.; Albrecht-Schmitt, T. E. *Angew. Chem., Int. Ed.* **2012**, *51* (8), 1869–1872. (j) Polinski, M. J.; Grant, D. J.; Wang, S.; Alekseev, E. V.; Cross, J. N.; Villa, E. M.; Depmeier, W.; Gagliardi, L.; Albrecht-Schmitt, T. E. *J. Am. Chem. Soc.* **2012**, *134* (25), 10682–10692. (k) Polinski, M. J.; Wang, S.; Cross, J. N.; Alekseev, E. V.; Depmeier, W.; Albrecht-Schmitt, T. E. *Inorg. Chem.* **2012**, *51* (14), 7859–7866.
- (9) Wang, S.; Alekseev, E. V.; Stritzinger, J. T.; Depmeier, W.; Albrecht-Schmitt, T. E. *Inorg. Chem.* **2010**, *49* (6), 2948–2953.
- (10) Gasperin, M. *Acta Crystallogr.* **1987**, *C43*, 2031–2033.
- (11) Gasperin, M. *Acta Crystallogr.* **1987**, *C43*, 1247–1250.
- (12) Gasperin, M. *Acta Crystallogr.* **1987**, *C43*, 2264–2266.
- (13) Gasperin, M. *Acta Crystallogr.* **1988**, *C44*, 415–416.
- (14) Gasperin, M. *Acta Crystallogr.* **1989**, *C45*, 981–983.
- (15) Gasperin, M. *Acta Crystallogr.* **1990**, *C46*, 372–374.
- (16) Behm, H. *Acta Crystallogr.* **1985**, *C41*, 642–645.
- (17) Wu, S.; Beermann, O.; Wang, S.; Holzheid, A.; Depmeier, W.; Malcherek, T.; Modolo, G.; Alekseev, E. V.; Albrecht-Schmitt, T. E. *Chem.—Eur. J.* **2012**, *18* (14), 4166–4169.
- (18) Wu, S.; Kegler, P.; Wang, S.; Holzheid, A.; Depmeier, W.; Malcherek, T.; Alekseev, E. V.; Albrecht-Schmitt, T. E. *Inorg. Chem.* **2012**, *51* (7), 3941–3943.
- (19) Duisenberg, A. J. M.; Kroon-Batenburg, L. M. J.; Schreurs, A. M. M. *J. Appl. Crystallogr.* **2003**, *36*, 220–229.
- (20) Sheldrick, G. M. *Acta Crystallogr.* **2008**, *A64*, 112–122.
- (21) High-Temperature and High-Pressure Crystal Chemistry. In *Reviews in Mineralogy & Geochemistry*; Hazen, R. M., Downs, R. T., Eds.; Mineralogical Society of America: Chantilly, VA, 2000; Vol. 41.
- (22) Werding, G.; Schreyer, W. Experimental studies on borosilicates and selected borates. In *Boron: Mineralogy, Petrology and Geochemistry*; Grew, E. S., Anovitz, L. M., Eds.; Reviews in Mineralogy; Mineralogical Society of America: Washington, DC, 2011; Vol. 33, pp 117–163.
- (23) Huppertz, H. *Chem. Commun.* **2011**, *47* (1), 131–140.
- (24) Emme, H.; Huppertz, H. *Acta Crystallogr.* **2004**, *C60*, i117–i119.
- (25) Huppertz, H.; Altmannshofer, S.; Heymann, G. *J. Solid State Chem.* **2003**, *170*, 320–329.
- (26) Huppertz, H.; Emme, H. *J. Phys.: Condens. Matter* **2004**, *16*, S1283–S1290.
- (27) Emme, H.; Weil, M.; Huppertz, H. *Z. Naturforsch.* **2005**, *60b*, 815–820.
- (28) (a) Piret, P.; Deliens, M. *Bull. Mineral.* **1982**, *105* (1), 125–128. (b) Demartin, F.; Diella, V.; Donzelli, S.; Gramaccioli, C. M.; Pilati, T. *Acta Crystallogr.* **1991**, *B47*, 439–446. (c) Alekseev, E. V.; Krivovichev, S. V.; Depmeier, W.; Siidra, O. I.; Knorr, K.; Suleimanov, E. V.; Chuprunov, E. V. *Angew. Chem., Int. Ed.* **2006**, *45* (43), 7233–7235.
- (29) (a) Williams, C. W.; Blaudeau, J.-P.; Sullivan, J. C.; Antonio, M. R.; Bursten, B.; Soderholm, L. *J. Am. Chem. Soc.* **2001**, *123*, 4346–4347. (b) Bolvin, H.; Wahlgren, U.; Moll, H.; Reich, T.; Geipel, G.; Fanghänel, T.; Grenthe, I. *J. Phys. Chem. A* **2001**, *105*, 11441–11445.
- (30) Wu, S.; Ling, J.; Wang, S.; Skanthakumar, S.; Soderholm, L.; Albrecht-Schmitt, T.; Alekseev, E.; Krivovichev, S.; Depmeier, W. *Eur. J. Inorg. Chem.* **2009**, No. 27, 4039–4042.
- (31) Unruh, D. K.; Baranay, M.; Baranay, M.; Burns, P. C. *Inorg. Chem.* **2010**, *49* (15), 6793–6795.
- (32) Weng, Z. H.; Wang, S.; Ling, J.; Morrison, J. M.; Burns, P. C. *Inorg. Chem.* **2012**, *51* (13), 7185–7191.
- (33) Brese, N. E.; O'Keeffe, M. *Acta Crystallogr.* **1991**, *B47*, 192–197.
- (34) Hughes, K. A.; Burns, P. C. *Am. Mineral.* **2003**, *88* (7), 962–966.
- (35) Burns, P. C.; Miller, M. L.; Ewing, R. C. *Can. Mineral.* **1996**, *34*, 845–880.
- (36) Piret, P.; Deliens, M.; Piretmeunier, J.; Germain, G. *Bull. Mineral.* **1983**, *106* (3), 299–304.
- (37) Ginderow, D.; Cesbron, F. *Acta Crystallogr.* **1985**, *C41*, 654–657.
- (38) Haberer, A.; Kaindl, R.; Konzett, J.; Glaum, R.; Huppertz, H. *Z. Anorg. Allg. Chem.* **2010**, *636*, 1326–1332.
- (39) Čejka, J. Infrared spectroscopy and thermal analysis of the uranyl minerals. In *Uranium: Mineralogy, Geochemistry and the Environment*; Burns, P. C., Finch, R., Eds.; Reviews in Mineralogy; Mineralogical Society of America: Washington, DC, 1999; Vol. 38, pp 521–622.
- (40) Neumair, S. C.; Kaindl, R.; Huppertz, H. *J. Solid State Chem.* **2012**, *185*, 1–9.
- (41) (a) Meinrath, G. *J. Radioanal. Nucl. Chem.* **1997**, *224*, 119–126. (b) Jeżowska-Trzebiatowska, B.; Bartecki, A. *Spectrochim. Acta* **1962**, *18*, 799–807. (c) Brint, P.; McCaffery, A. *J. Mol. Phys.* **1973**, *25*, 311–

322. (d) McGlynn, S. P.; Smith, J. K. *J. Mol. Spectrosc.* **1961**, *6*, 164–187.
- (42) Meinrath, G. *J. Radioanal. Nucl. Chem.* **1997**, *224*, 119–126.
- (43) Wu, S.; Wang, S.; Polinski, M. J.; Depmeier, W.; Albrecht-Schmitt, T. E.; Alekseev, E. V. *Z. Kristallogr.* **2013**.